Int. J. Electrochem. Sci., 10 **(2015)** 504 - 518

International Journal of
ELECTROCHEMICAL
SCIENCE
www.electrochemsci.org

Corrosion Inhibition of Aluminium Alloy in Alkaline Media by Neolamarkia Cadamba Bark Extract as a Green Inhibitor

Namrata Chaubey[1], *Vinod Kumar Singh*[1], *Savita*[1], *M. A. Quraishi*[2,*] *Eno E. Ebenso*[3,4]

[1]Department of Chemistry, Udai Pratap Autonomous College, Varanasi-221002, India
[2]Department of Chemistry, Indian Institute of Technology (Banaras Hindu University), Varanasi-221005, India.
[3] Department of Chemistry, School of Mathematical and Physical Sciences, North-West University (Mafikeng Campus), Private Bag X2046, Mmabatho 2735, South Africa
[4]Material Science Innovation & Modelling (MaSIM) Focus Area, Faculty of Agriculture, Science and Technology, North-West University (Mafikeng Campus), Private Bag X2046, Mmabatho 2735, South Africa
[*]E-mail: maquraishi.apc@itbhu.ac.in; maquraishi@rediffmail.com

Received: 1 October 2014 / *Accepted:* 26 November 2014 / *Published:* 2 December 2014

The aqueous extract of *Neolamarkia Cadamba* (NC) bark was investigated as corrosion inhibitor for aluminium alloy (AA) in 1 M NaOH solution. The techniques employed for corrosion inhibition are weight loss, polarization resistance, Tafel polarization and electrochemical impedance spectroscopy (EIS). The inhibition efficiency increases with increasing the concentration and shows maximum inhibition efficiency (87 %) at optimum concentration (0.6 g/L). Polarization study revealed that it is a mixed type inhibitor. The existence of protective film on the surface of AA was confirmed by the scanning electron microscope (SEM).

Keywords: Aluminium alloy; Neolamarkia Cadamba; Corrosion inhibitor; SEM; EIS

1. INTRODUCTION

Due to the high technological values and many industrial applications, aluminum and its alloys represent an important category of materials. It is an attractive anode material for energy storage and conversion because of its high specific capacity, highly negative standard electrode potential and environmentally benign characteristics [1]. Consequently, the aluminium behavior has an import impact on the battery properties. The corrosion behavior of AA in alkaline media has been extensively studied in the development of aluminium anode for aluminium/air batteries [2-9]. The protection of

AA from corrosion in several media is mainly depends on the natural oxide surface. The alkaline solution, are known to render the oxide film non-protective; because OH^- ion dissolves this surface oxide film and metal surface establishes a very negative potential, with the formation of aluminate ion [10]. For the protection of AA from corrosion, it is necessary to add corrosion inhibitors in alkaline media. The addition of inhibitors helps to improve the efficiency in devices such as Aluminium-alkaline battery [11].

A survey of literature indicates that various organic and inorganic corrosion inhibitors [12-15] are widely used to prevent the dissolution of aluminium in alkaline media. However, most of them are expensive, non-biodegradable and toxic to the environment and thus the corrosion inhibition process by using these chemical inhibitors is limited due to environmental regulation. In view of this, it is worthwhile to pay heed towards a very cheap and environmentally safe research for corrosion inhibition of aluminium in alkaline solution. In order to achieve the above goal extracts of various parts of plants (leaves, stem, bark, fruit etc) have been used as corrosion inhibitor because they are incredibly rich source of naturally synthesized organic compounds that can be extracted using simpler techniques with low cost.

Plant extracts have been choosen because they are environmentally acceptable, readily available and renewable source for a wide range of needed inhibitors. In this study, we have taken bark of *Neolamarckia Cadamba* tree as an inhibitor for AA in 1 M NaOH solution. *Neolamarckia Cadamba* (*f.* Rubiaceae), commonly called kadamba is an evergreen, tropical tree native to the India. It is frequently found all over the India on the slopes of evergreen forests up to 500 m. It is found in the sub-himalayan tract from Nepal eastwards on the lower hills of Darjeeling terai in West Bengal where it is common; in Chota Nagpur (Bihar), Orissa and Andhra PradeshPradesh, in the Andamans, it is very common in damp places along large streams, and in Karnataka and Kerala on the west coast, and western ghats at low level in wet places. It is also distributed in Thailand and Indo-china and east-ward in Malaysian archipelago to Papua New Guinea [16-18]

In present study, we are focused on the corrosion inhibition performance of aqueous extract of *Neolamarckia Cadamba* bark on AA in 1 M NaOH solution. The inhibiting study was conducted by weight loss measurement, open circuit potential (OCP) vs. time measurements, potentiodynamic polarization, linear polarization resistance and electrochemical impedance spectroscopy.

2. EXPERIMENTAL STUDY

2.1 Specimens and electrolyte

The aluminium alloy was purchased from the market and analyzed in Department of metallurgical engineering, IIT (BHU). The composition (wt %) of the AA specimen used was: Si = 0.77, Fe=0.93, Cu=0.02, Mn=0.11, Mg=0.01, Zn=0.01, Cr=0.05, Ti=0.02, V=0.01, Ga=0.01 and balance Al. The test solution 1M NaOH was prepared by dissolving 40 gram of NaOH in 1000 ml of double distilled water.

2.2 Preparation of extract solution

Neolamarkia Cadamba barks were collected, dried and powdered. 1g of powder was taken in round bottom flask containing 100 ml 1M NaOH and reflux for 1 h. Thereafter the mixture was cooled and filtered. The residue of mixture was dried and weighed. The volume of the filtrate was maintained up to 100 ml. The concentration of the solid residue dissolved in 1M NaOH was 1000 mg/L and this solution was used as a stock solution.

2.3 Gravimetric measurement

Specimen with dimension 2.5 × 2.0 × 0.035 was used in gravimetric measurement. The aluminium coupons were abraded with emery paper having the grade of 600, 800 and 1000, degreased with acetone and then washed with distilled water. In weight loss measurement, every coupon was weighed through an electronic balance and then placed in 100 ml of test solution for 3 hour at 303 K. After immersion time, the sample was withdrawn from the solution, washed with distilled water and cleaned with acetone, dried and weighed. The same process was repeated at different temperature (313, 323 and 333 K).The corrosion rate of aluminium was calculated using the following equation:

$$C_R = \frac{87.6 \times W}{ATD} \quad (1)$$

where, C_R is the corrosion rate expressed in mm/year, W is used for weight loss of metal (mg), T is the exposure time and D is the density of aluminum (2.7 $g\ cm^{-3}$).

The surface coverage (θ) and inhibition efficiency (η %) was also calculated by following equation:

$$\eta\% = \frac{w_o - w_i}{w_o} \times 100 \quad (2)$$

$$\theta = \frac{w_o - w_i}{w_o} \quad (3)$$

where, w_0 and w_i are the weight loss value in the absence and presence of inhibitor, respectively.

2.4 Electrochemical measurement

The electrochemical measurement was carried out by using three-electrode cell assembly at room temperature. These three electrode cell is connected with the Gamry Potentiostat/Galvanostat (Model 300) instrument and all the experiment is carried out with this software. AA of 7.5 cm long specimen with an exposed area of 1 cm^2 was used as a working electrode. The rest of area is coated with commercially available lacquer. A platinum wire and a saturated calomel electrode (SCE) i.e. (Cl^- | (4M) Hg_2Cl_2 (*s*)| Hg (*l*) | Pt) were used as counter and reference electrodes respectively. All the tests were performed after 15 minute immersion of AA in the absence and presence of inhibitors at different concentrations in 1 M NaOH solution.

The open-circuit potential (OCP) of the working electrode was recorded as a function of time for 200s. To obtain steady state open-circuit potential (OCP), the working electrode was immersed in test solution (1 M NaOH) for approximately 15 minutes before starting the electrochemical measurement. EIS measurements were performed in the frequency range of 100000-0.01 Hz using AC signal at OCP. The values of charge transfer resistance (R_{Ct}) and double layer capacitance (C_{dl}) were evaluated from Nyquist and Bode plots [19].

Linear polarization study was performed from the cathodic potential of -0.02 V to anodic potential of +0.02 V vs OCP at a scan rate of 0.125 mV/s. Potentiodynamic polarization curves were obtained by scanning the electrode potential from -250 to +250 vs corrosion potential (E_{corr}) at a sweep rate of 1 mV/sec [20].

2.5 Surface characterization

AA coupons with the size of 2 × 2.5 × 0.046 were immersed in the absence and presence of optimum concentration of inhibitor for 3 h. after that the coupons were taken, washed with distilled water and rinsed using acetone. After drying, coupons were cut into dimension of 1 cm^2 and then investigate using SEM technique.

3. RESULT AND DISCUSSION

3.1 Gravimetric measurement

3.1.1 Inhibitor concentration

Weight loss study was carried out for 3 hour immersion time at different concentration. As the concentration of inhibitor increases, the inhibition efficiency (η %) also increases and the corrosion rate decreases. The bark extract shows maximum inhibition efficiency (87%) at 0.6 g/L after that increasing concentration does not increase the inhibition efficiency. The percentage inhibition efficiency (η %) and corrosion rate (C_R) are shown in Table (1).

Table 1. Inhibition efficiency (η%) and corrosion rate (C_R) values obtained from gravimetric measurement for AA in 1M NaOH containing various concentrations of the inhibitors at 303K

Inhibitors	C_{inh} (g/L)	C_R (mm/year)	Θ	η (%)
Blank	0.0	351.0	--	--
NC	0.2	169.7	0.27	64.6
	0.4	99.4	0.57	74.7
	0.5	46.5	0.80	82.56
	0.6	30.2	0.87	87.1

3.1.2 Effect of temperature

With the concentration, temperature also affects the percentage inhibition efficiency. As the fig.1 shows, C_R increases and η % decreases from 87 to 78% at increasing temperature from 303 to 333 K with but it did not decrease markedly up to 333K. This may be due to the partial desorption of the inhibitor from AA surface with temperature.

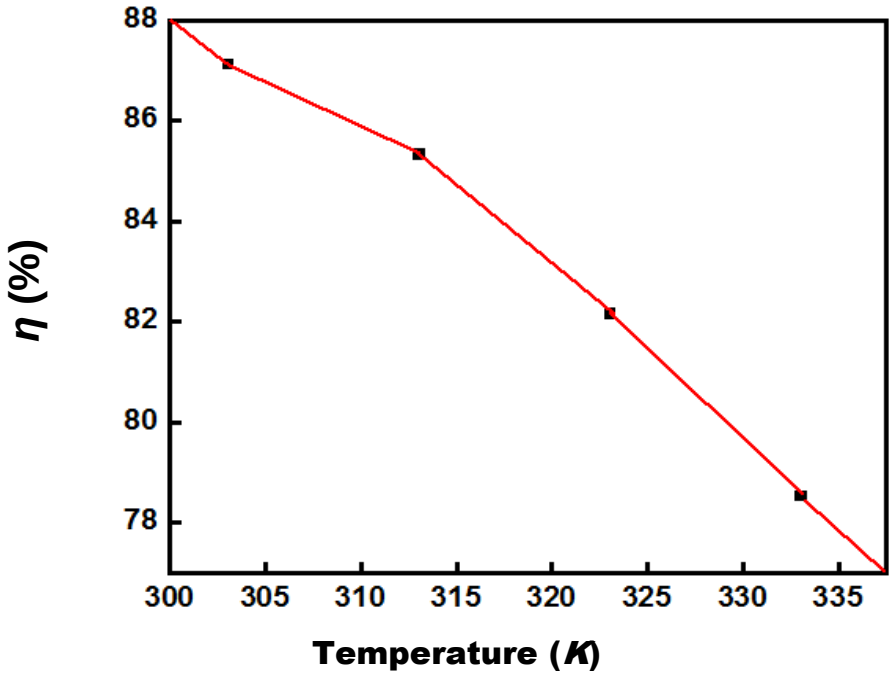

Figure 1. Inhibition efficiency of Neolamarkia Cadamba barks extract at different temperatures.

The values of C_R with η % at different temperatures are reported in Table.2

Table 2. The corrosion rate values obtained for AA in 1 M NaOH in the absence and presence of inhibitor at different temperature.

Inhibitor	Temperature (K)	C_R (mm/year)	η (%)
Blank	303	351.0	--
	313	528.1	--
	323	885.6	--
	333	1127.2	--
NC	303	30.2	87.1
	313	51.9	85.3
	323	105.9	82.1
	333	162.2	78.5

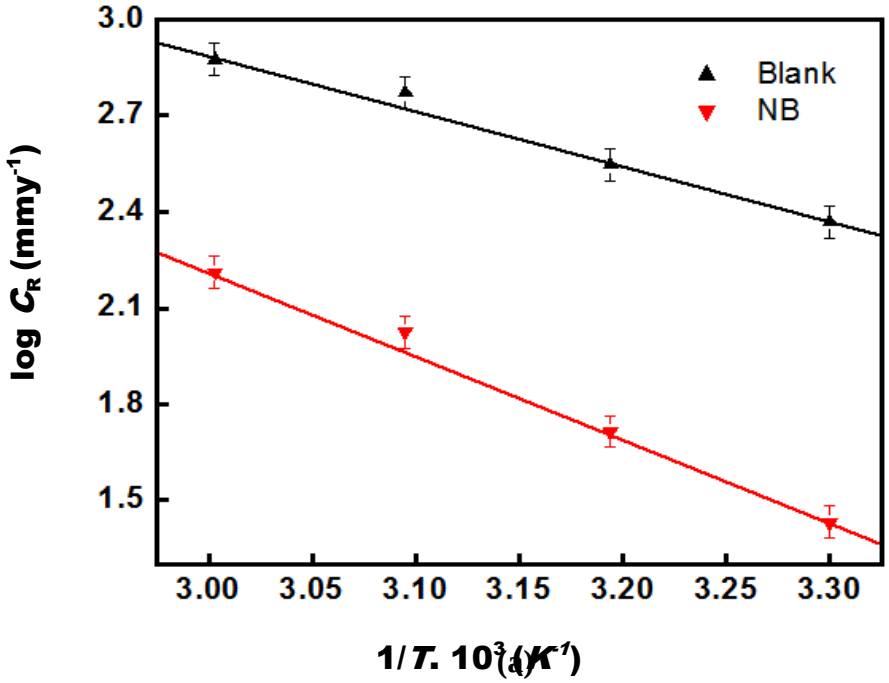

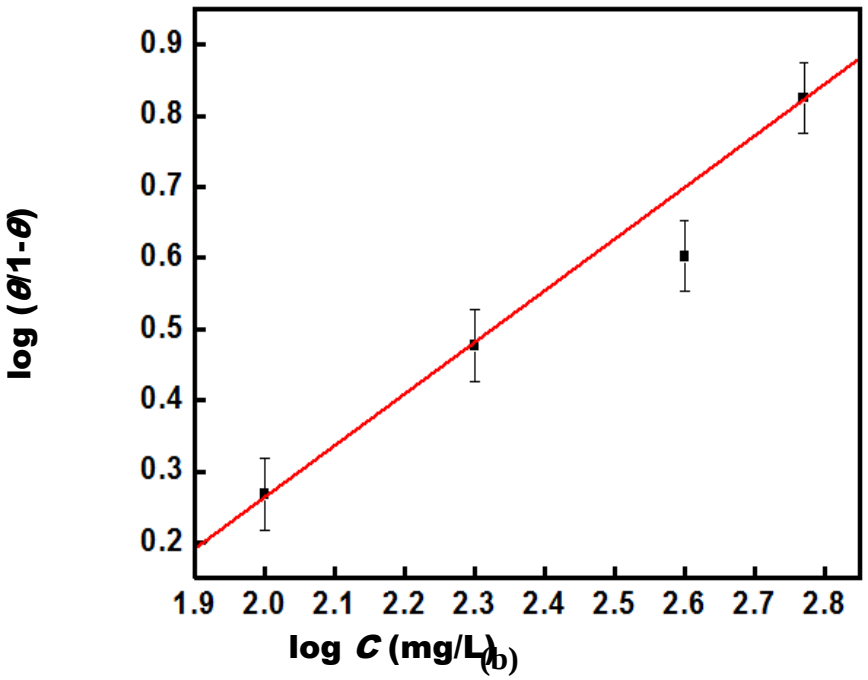

Figure 2 (a). Arrhenius plots for AA corrosion rates (C_R) in 1 M NaOH without and with the Neolamarkia Cadamba barks extract. **(b):** Langmuir isotherm plots for adsorption of inhibitor on AA in 1 M NaOH.

It has been shown that the logarithm of corrosion rate is a linear function with 1/*T*. The apparent activation energy (*E*a) for corrosion process of AA in 1 M NaOH solution is calculated by the following equation:

$$\log C_R = \frac{-Ea}{2.303RT} + \lambda \quad (4)$$

where *E*a is the apparent activation energy of the corrosion process, *R* is the general gas constant, and *A* is the Arrhenius pre-exponential factor. The values of *E*a were determined by the slope value which is obtained by using a plot between log of corrosion rate and 1/*T* (Fig.2). This plot gives a straight line as shown in with a slope of *E*a/2.303*R*. The *E*a values for without and with the inhibitor are 33.6 KJ/mol and respectively. It can be clearly seen that the E_a values for inhibited systems were higher than the uninhibited 1M NaOH which suggest the formation of an energy barrier for mass and charge transfer in inhibited system. The adsorbed inhibitor molecules on the metal surface raise the energy of activation for charge and mass transfer.

3.1.3 Adsorption isotherm

Adsorption characteristics are very useful to understand the nature of corrosion inhibition and it can be deduced in the term of adsorption isotherm. By fitting the various adsorption isotherms including Freundlich, Temkin, and Langmuir and Frumkin isotherms, the data were tested graphically. In this section, the best fitted isotherms that describe the adsorption behavior of plant leaves extract on aluminium surface was Langmuir adsorption isotherm and it can be expressed by using following equation:

$$K_{ads}C = \frac{\theta}{1-\theta} \quad (5)$$

where K_{ads} is the adsorption equilibrium constant, *C* denotes the concentration of the inhibitors. On plotting log θ / (1–θ) versus log *C*, a straight line was obtained as shown in Fig.2 (b). This indicates that the bark extract as inhibitor obeyed Langmuir adsorption isotherm [21].

The adsorption equilibrium constant (*K*ads) is associated with standard free energy of adsorption Δ*G* (ads) by the following equation:

$$K_{\text{ads}} = \frac{1}{C_{(sol.)}} \exp\left(\frac{\Delta G^{\circ}_{\text{ads}}}{RT}\right) \quad (6)$$

Where R is universal gas constant, *T* is the absolute temperature and *C* is the concentration of water (1000 g/L). The values of *K*ads is representing here in g/L, thus in this equation, the concentration of water is taken in g/L in the place of 55.5 mole/L.

The values of *K* (ads) and Δ*G* (ads) were calculated and given in Table.3. It is seen that the negative value of Δ*G* is found in all cases. The spontaneity of the adsorbed species and their stability on the aluminium surface is confirmed by the negative value of Δ*G*. In present case, the value of Δ*G*ads for the inhibited system is -24 kJmol^{-1} occurs which is less than -40 kJ mol^{-1} that signifies physisorption. The K_{ads} values reduced with increasing temperature, it indicates enhancing desorption process at elevated temperatures.

Table 3. Thermodynamic parameters obtained for adsorption of inhibitor on AA in 1 M NaOH at different temperature.

Inhibitor	Temperature	K_{ads} (g^{-1})	G^{o}_{ads} ($KJmol^{-1}$)	H (%)
NC	303	11.2	-23.5	87.1
	313	9.4	-23.8	85.3
	323	7.6	-23.9	82.1
	333	5.9	-24.0	78.5

3.2 Electrochemical measurement

3.2.1 Polarization study

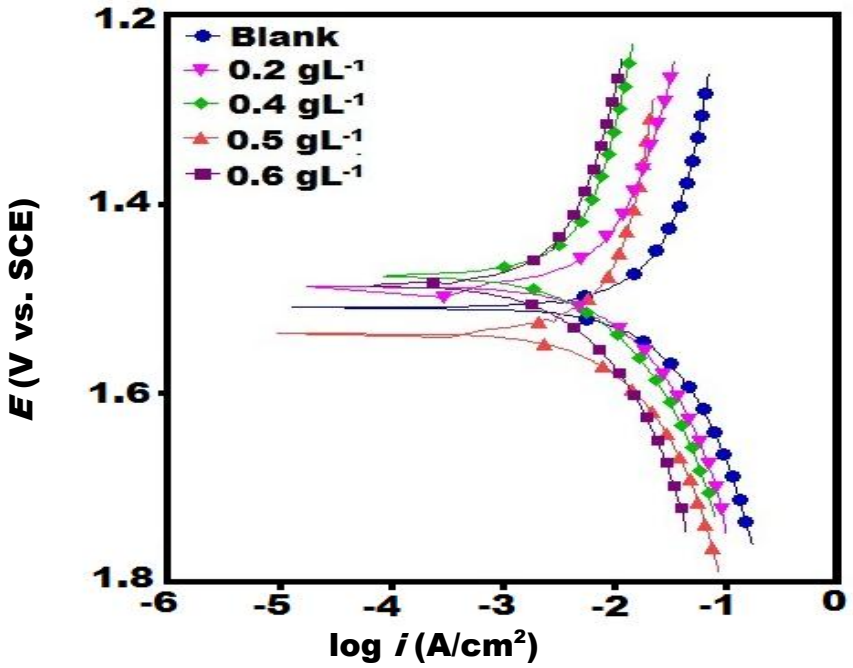

Figure 3. Tafel polarization curve for AA in 1 M NaOH without and with the different concentration of *Neolamarkia Cadamba* barks extract.

Tafel polarization curve for AA in 1 M NaOH solution with the different concentration of inhibitor are shown in Fig.3. The anodic and cathodic current-potential curves were extrapolated up to their intersection at the point where corrosion current density (I_{corr}) and corrosion potential (E_{corr}) were obtained [22]. Anodic and cathodic curves both are affected by the addition of inhibitors. It can be observed in the fig that current density decreases with increasing the concentration of inhibitor and lowest current density was observed at optimum concentration (0.6 gL^{-1}). From the Table.4, values of electrochemical parameters i.e. corrosion potential (E_{corr}), corrosion current density (I_{corr}), anodic Tafel

constant (β_a), cathodic Tafel constant (β_c), polarization resistance (R_P) along with percentage inhibition efficiency (η %) were obtained.

The inhibition efficiency with corrosion current density and polarization resistance is calculated from following equation:

$$\%IE = \frac{I^0_{corr} - I_{corr}}{I^0_{corr}} \times 100 \quad (7)$$

$$\%IE = \frac{R_{p(inh)} - R_p}{R_{p(inh)}} \times 100 \quad (8)$$

Where I^0_{corr} and I_{corr} are the corrosion current density and R_p and $R_{p\ (inh)}$ is polarization resistance with or without inhibitor. Table.4 indicates an increase in R_p values in the inhibited system compared with those in the uninhibited one, which suggests AA corrosion is reduced in the inhibited system relative to the uninhibited system [23]. The highest R_p value (12.64 Ωcm^2) was obtained at 0.6 g/L concentration of *NC* bark extract suggesting the formation of its adherent protective film on the metal surface.

It can be seen from the table that the difference in the values of β_a and β_c is not more in the presence of inhibitor indicating that the studied inhibitor is of mixed-type [24].

Table 4. Electrochemical polarization parameters for AA in 1 M NaOH in the absence and presence of different concentrations of inhibitor at 308 K

Inhibitor	Tafel polarization				Linear polarization				
	I_{corr} ($mAcm^{-2}$)	E_{corr} (V/SCE)	β_a (V/dec)	β_c (V/dec)	C_R ($mpy\times10^3$)	η (%)	R_p (Ωcm^{-2})	θ	η *(%)*
Blank	96.3	-1.508	1.001	0.504	41.3	--	1.279	--	--
0.2 g/L	25.40	-1.490	6.115	0.309	10.92	73.62	5.57	0.781	78.18
0.4g/L	18.60	-1.495	4.132	0.251	7.97	80.68	5.84	0.793	79.31
0.5g/L	10.30	-1.473	2.17	0.173	4.42	89.30	7.78	0.844	84.41
0.6g/L	8.16	-1.480	1.715	0.152	3.50	90.62	12.64	0.904	90.40

3.2.2 Impedance measurement

The corrosion behavior of AA in 1 M NaOH solution in the absence and presence of different concentration of inhibitors was also investigated by impedance spectra. The impedance spectra is recorded and displayed in the form of Nyquist plot shown in the Fig.4. As can be seen in fig, this plot consists of depressed semicircles indicating that the corrosion process is mainly charge transfer controlled [25]. The depressed semicircle comes because of inhomogeneous surface associated with the metal surface [26]. These curves are identical in shape and having large capacitive loop at higher frequencies (HF), inductive loop at intermediate frequencies (IF) and a second capacitive loop at lower frequencies (LF) value [27]. Various literatures have been known for the similar results of AA in alkaline media [28, 29].

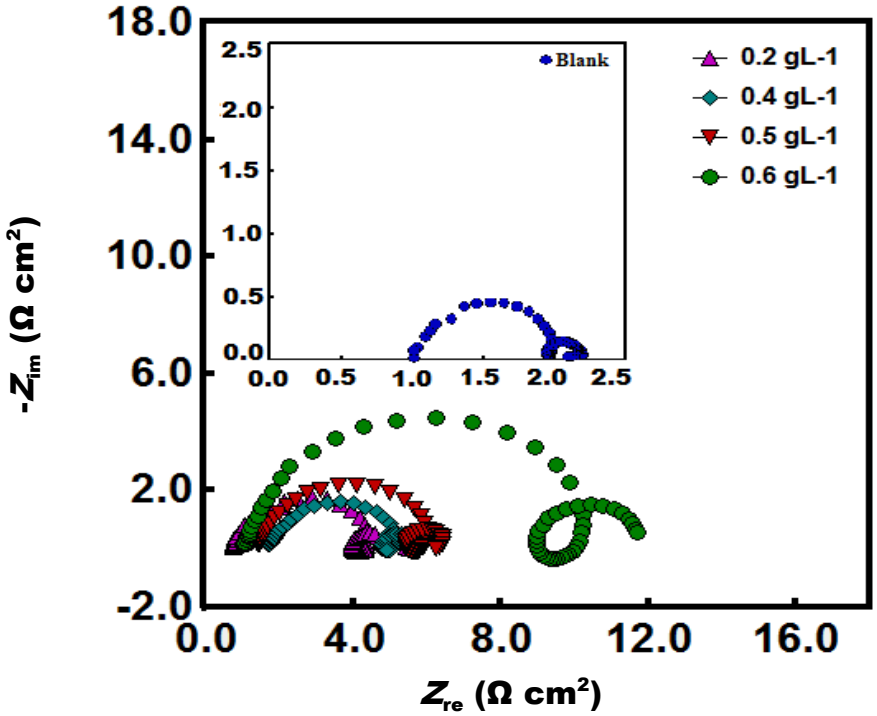

Figure 4. Nyquist plots for AA in 1M NaOH in absence and presence of different concentrations of inhibitor at 308 K.

The HF capacitive loop is attributed to the presence of oxide layer. According to Brett [30, 31], first capacitive loop is described by the reaction of aluminium oxidation at the metal/oxide/electrolyte interface. This process involves the migration of Al^{+} through the oxide/ solution interface where they are oxidized to Al^{3+}. At this interface, OH^{-} and O^{2-} are also formed. The explanation for IF inductive loop is that it may be due to the relaxation process in the protective (oxide) layer by the intermediate adsorbed species such as OH^{-} [32]. The second LF capacitive loop is originated due to metal dissolution [33].

The impedance parameters are shown in Table.5 and these parameters are analyzed by fitting the equivalent circuit given in Fig.5. The circuit is composed of solution resistance (*R*s), charge transfer resistance (R_{CT}) parallel to constant phase element (*CPE*), inductance (*L*) and R_L. The *CPE* is used in the place of capacitor to fit the semicircle more accurately and is defined by the components Y_O and n which is expressed by the following relation [34]:

$$Z_{CPE} = Y_o^{-1}(j\omega)^{1-n} \quad (9)$$

where Y_0 is the admittance, ω is angular frequency ($\omega = 2\pi f_{max}$) at which the imaginary part of the impedance (-Zim) is maximal and f_{max} is AC frequency at maximum, *n* is used for the phase shift, which can be used as a gauge of the heterogeneity or roughness of the mild steel surface. *CPE* can be described by the varied n values. Depending on *n*, *CPE* can represent resistance ($Y_0 = R$, n = 0), capacitance ($Y_0 = C$, $n = 1$), inductance ($Y_0 = L$, $n = -1$) or Warburg impedance ($n = 0.5$, Y_0 =W) [35].

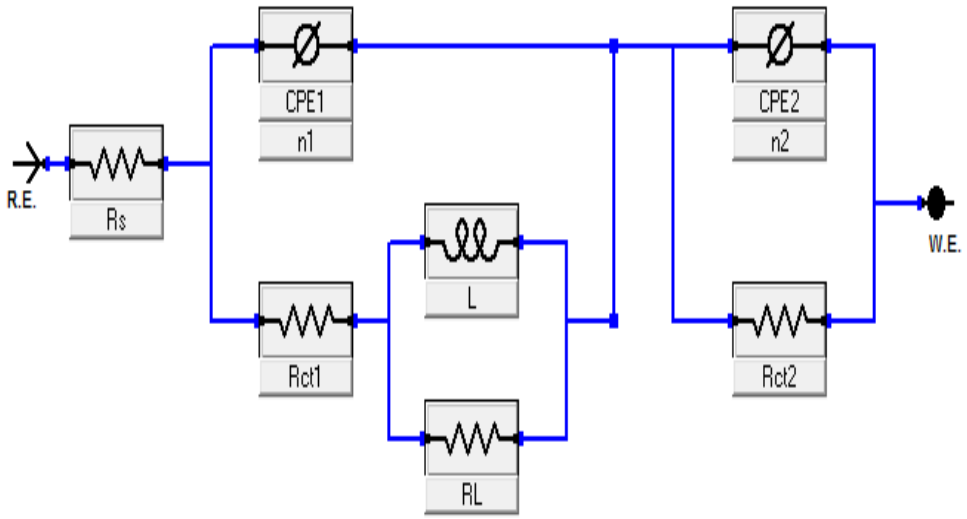

Figure 5. Equivalent circuit used to fit the impedance spectra.

Table 5. Electrochemical impedance parameters for AA in 1 M NaOH in the absence and presence of different concentration of inhibitor.

Inhibitor	R_s (Ω)	Q_1 ($S\Omega^{-1}cm^2$)	n_1	$(R_{ct})_1$ (Ωcm^2)	L (Hcm^2)	R_L (Ωcm^2)	Q_2 ($S\Omega^{-1}cm^2$)	n_2	$(R_{ct})_2$ ($\Omega\ cm^2$)	C_{dl} ($\mu F\ cm^{-2}$)	$\eta\ \eta$ (%) η
Blank	1.023	500×10^{-6}	0.975	0.849	0.221	0.121	39.8×10^{-6}	5.211	0.188	413.8	--
0.2 g/L	0.648	165.7e-6	0.932	2.635	0.011	1.451	1.006	2.732	1.006	118.3	68.0
0.4g/L	0.784	194.1e-6	0.925	2.812	0.016	1.357	1.713	2.357	1.713	100.5	77.89
0.5 g/L	1.468	99.08e-6	0.956	3.322	0.003	1.163	0.579	3.224	0.579	76.7	86.66
0.6 g/L	1.060	176.5e-6	0.891	8.136	0.046	2.285	2.486	2.949	2.486	43.9	89.62

The pronounced effect was observed in the values of R_{CT} the presence of inhibitor (Table.5). It increases with increasing the concentration and maximum value of R_{CT} was found at 0.6 g/L (optimum concentration). This increase may be due to the formation of protective film at metal/solution interface. From Table.5, it can be clearly seen that C_{dl} decreased with addition of inhibitor and this decrease in C_{dl} may be attributed to the decrease in local dielectric constant or increasing thickness of the electrical double layer suggesting the inhibiting action on metal/ solution interface [36].

The C_{dl} may be calculated by the following equation :

$$C_{dl} = Y_0(\omega_{max})^{n-1} \quad (10)$$

Here, ω_{max} is the frequency at which imaginary element reaches a maximum.

The table reveals that the value of R_{CT} increases with increasing the concentration and the highest value (8.13 Ωcm^2) obtained at 0.6 g/L (optimum concentration).

The inhibition efficiency, η (%), is calculated from R_{CT} values as given in equation [37]:

$$\%IE = \frac{R_{CT}^{-1} - R_{CT(inh)}^{-1}}{R_{CT}^{-1}} \times 100 \quad (11)$$

Where R_{CT}^{-1} and $R_{CT}^{-1}{}_{(inh)}$ are the charge transfer resistance values without and with inhibitor, respectively

Fig (6) showed the bode impedance and phase angle plot for AA in 1 M NaOH without and with the various concentrations of inhibitor. For ideal Capacitor, the value of slope value (*S*) and pkase angle (α) should be -1 and -90^0 respectively [38]. This response is a characteristic of capacitive behavior. In this case, maximum S value is 0.68 and phase angle is 58^0 observed. These deviations considered to be the deviation from the ideal capacitive behavior [39].

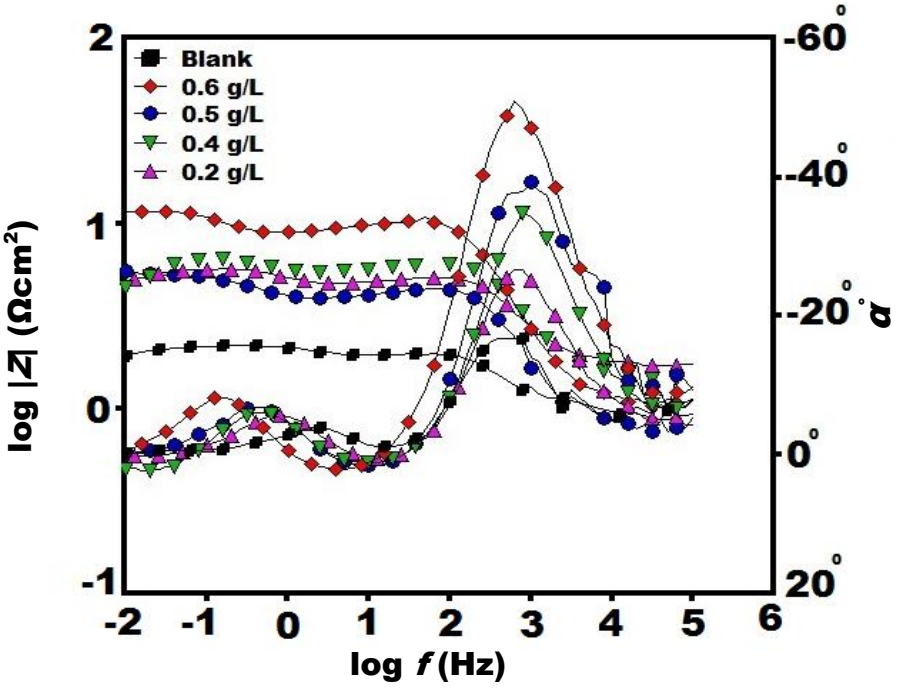

Figure 6. Bode (log f vs. log |Z|) and phase angle (log f vs. α) plots of impendence spectra for AA in 1M NaOH in absence and presence of different concentrations of inhibitors at 308 K.

3.2.3. Scanning electron microscope

SEM images of the surface of AA in 1 M NaOH without and with the presence of optimum concentration of inhibitor are recorded and shown in Fig.7(a-b). There is much difference occur in both images. Fig.7(a) is for uninhibited AA surface in NaOH which is highly damaged and more roughness occur in it. After adding inhibitor smoothness occurs in Fig.7 (b) due to the formation of protective layer on AA surface.

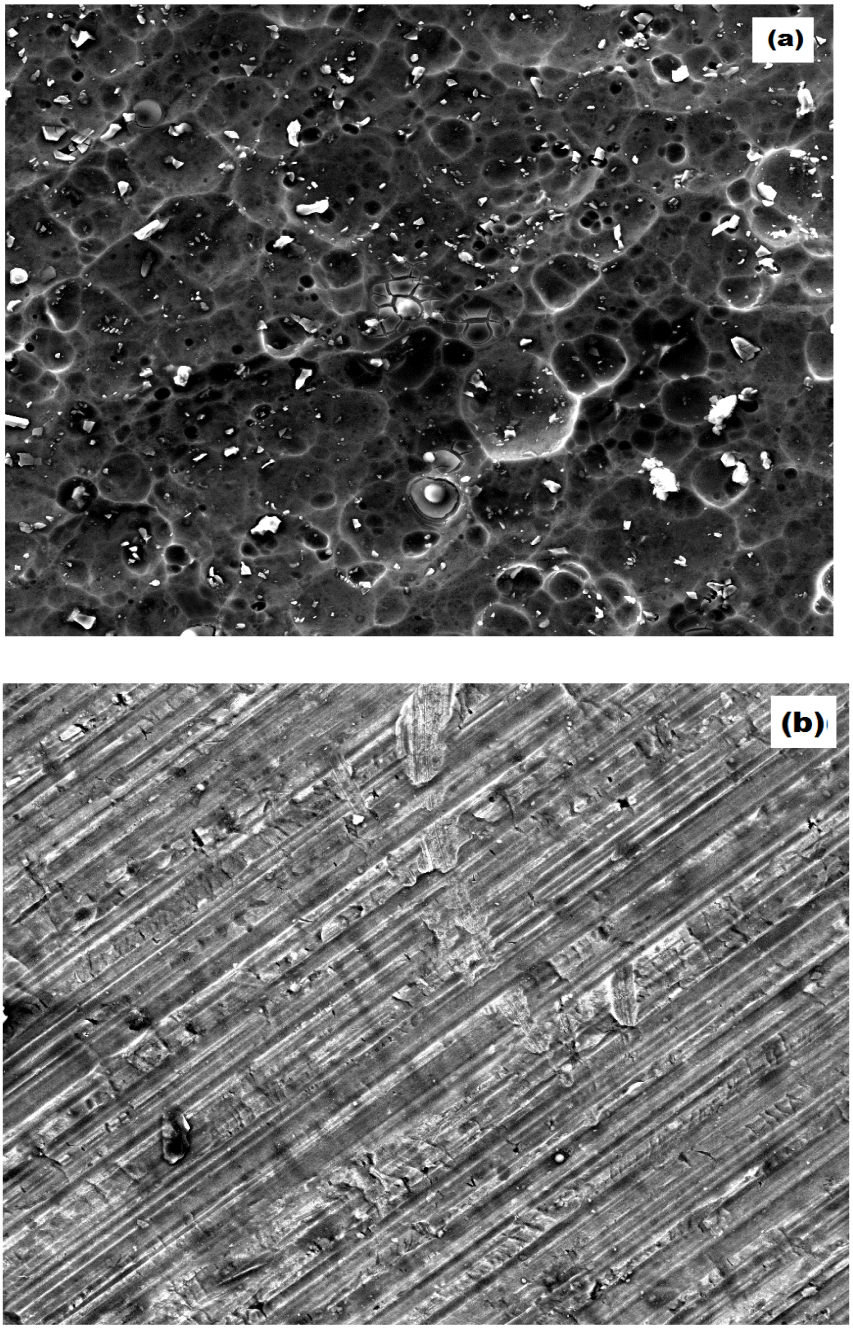

Figure 7. SEM micrographs of AA surface (a) AA in 1 M NaOH, (b) Inhibited AA (1 M NaOH + 0.6 g/L of NC bark extract).

3.3. Inhibitor constituents

To understand the adsorption process of inhibitor molecules, it is important to having knowledge of their inhibiting action on corrosion. The chemical constituents present in Neolamarkia Cadamba are tannins [40] and a new pentacyclic triterpenic acid isolated from the stem bark Neolamarckia Cadamba named cadambagenic acid (18α-olean-12ene-3β-hydroxy 27, 28-dioic acid) along with this acid quinovic acid and β- sitosterol (Fig.8) have also been isolated [41,]. From the fig

of constituents, it is clear that these constituents having Π bonds and heteroatom (Oxygen). Therefore, the adsorption process occurs either by the electrostatic interaction in charged molecule and constituents of inhibitors or by the interaction of unshared electron pairs of inhibitor molecules.

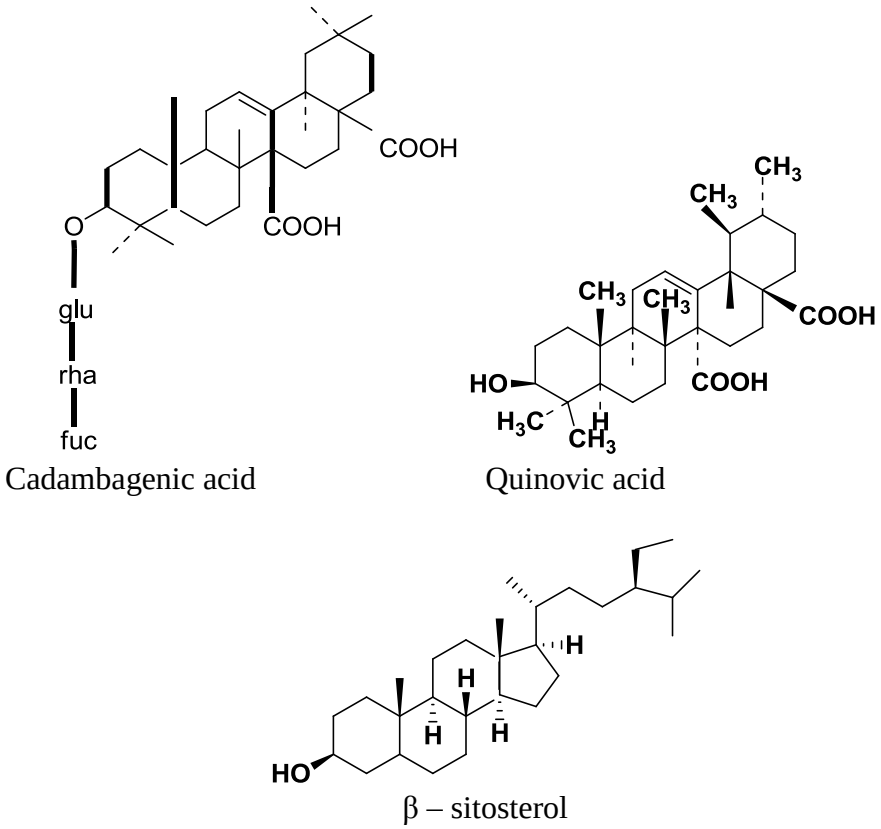

Cadambagenic acid Quinovic acid

β – sitosterol

Figure 8. Chemical constituents present in *neolamarkia cadamba* bark**.**

4. CONCLUSION

Neolamarckia Cadamba bark extracts proved to be a good corrosion inhibitor for AA in 1 M NaOH solution. The inhibition efficiency increases with increasing the extract concentration and decreases with increasing temperature.

The adsorption of bark extract on AA surface followed the Langmuir adsorption isotherm.Polarization study reveals that it is a mixed type inhibitor.

ACKNOWLEDGEMENTS
Authors are highly thankful to Prof. M. A. Quraishi, Head, Departement of Chemistry, I.I.T. (B.H.U.) for providing facilities for successful completion of my research work.

References

1. R. Mori, *RSC Advances* 3 (2013) 11547
2. S. Zaromb, *J. Electrochem. Soc.* 109 (1962) 1125.
3. L. Bocksite, D. Trevethan, S. Zaromb, *J. Electrochem. Soc.* 110 (1963) 267.
4. C.D.S. Tuck, J.A. Hunter, G.M. Scamans, *J. Electrochem. Soc*. 134 (1987) 2970.
5. S. Real, M.U. Macdonald, D.D. Macdonald, *J. Electrochem. Soc.* 135 (1988) 2397.
6. I.J. Albert, M.A. Kulandainathan, M. Ganesan, V. Kapali, *J. Appl. Electrochem.* 19 (1989) 547.
7. D. Chu, R.F. Savinel, *Electrochim. Acta* 36 (1991) 1631.
8. K.Y. Chan, R.F. Savinell, *J. Electrochem. Soc.* 138 (1991) 1976.
9. W. Wilhelmsen, T. Arnesen, O. Hasvold, N.J. Storkersen, *Electrochim. Acta* 36 (1991) 79
10. H.N. Soliman, *Corrosion Science* 53 (2011) 2994.
11. D. Mercier, M.-G. Barthés-Labrousse, *Corros. Sci.* 51 (2009) 339.
12. O.K. Abiola, J.O.E. Otaigbe, O.J. Kio, *Corros. Sci*. 51 (2009) 1879.
13. D. Mercier, M.-G. Barthés-Labrousse, *Corros. Sci*.51 (2009) 339.
14. J. Zhang, M. Klasky, B.C. Letellier, *J. Nucl. Mater*. 384 (2009) 175.
15. H.B. Shao, J.M. Wang, Z. Zhang, J.Q. Zhang, C.N. Cao, *Mater. Chem. Phys.* 77 (2002) 305.
16. A. Dubey, S. Nayak and D. C. Goupale *Der Pharmacia Lettre*, 3 (2011) 45.
17. Prajapati, Purohit, Sharma and kumar, *Agrobios (India) publisher Jodhpur*, (2007) 52.
18. The wealth of India, *NISCAIR press publishers*, New Delhi, (2006) 305.
19. M.A. Quraishi, D. K. Yadav and I. Ahamad, *The Open Corrosion Journal*, 2 (2009) 56.
20. Ambrish Singh, I. Ahamad, D. K. Yadav, V. K. Singh & M. A. Quraishi, *Chemical Engineering Communications* 199:1, (2012) 63.
21. AS Algaber, M. El-Nemma Eman, *Mater Chem Phys* 86 (2004) 26.
22. D. K. Yadav , M.A. Quraishi , B. Maiti, *Corrosion Science*. 55 (2012) 254.
23. D. K. Yadav and M. A. Quraishi *Ind. Eng. Chem. Res*. 51 (2012) 14966.
24. M.A. Quraishi, K.R Ansari, D. K. Yadav, Eno E. Ebenso *Int. J. Electrochem. Sci.* 7 (2012) 12301.
25. C. Montecelli, F. Zucchi, G. Brunoro, G. Trabanelli, *J. Appl. Electrochem*. 27 (1997) 325.
26. M.S. Morad, *Mater. Chem. Phys*. 60 (1999) 188.
27. Brett, C.M.A., *J. Appl. Electrochem*. 20 (1990) 1000.
28. Abdel-Gaber, A.M., Khamis, E., Abo-EIDahab, Sh., Adeel, H., *Mat. Chem. Phys*. 109 (2008) 297.
29. H.B. Shao, J.M. Wang, Z. Zhang, J.Q. Zhang, C.N. Cao, *Mat. Chem. Phys*. 77 (2003) 305.
30. Brett, C.M.A., *J. Appl. Electrochem*. 20 (1990) 1000.
31. Brett, C.M.A., *Corros. Sci.* 33, (1992) 203.
32. Lorenz, W.J., Mansfeld, F., *Corros. Sci.* 21(1981) 647.
33. S.S.A. Rehim, H.H. Hamdi, A.A.Mohammed, *Appl. Surf. Sci.* 187 (2002) 279.
34. A.K. Singh, M.A. Quraishi, *Corros. Sci.* 52 (2010) 1373.
35. D. K. Yadav and M. A. Quraishi *Ind. Eng. Chem. Res*. 51 (2012) 8194.
36. A.Y. Musa, R.T.T. Jalgham and A. B. Mohamad, *Corros. Sci*. 56 (2012) 176.
37. D. K. Yadav, D.S. Chauhan, I. Ahamad and M.A. Quraishi RSC Advances, 3 (2013) 632.
38. K.R. Ansari, M.A. Quraishi, *Journal of Industrial and Engineering Chemistry*,20 (2014) 2819-2829.
39. K.R. Ansari, M.A. Quraishi, Prashant, Eno E. Ebenso *Int. J. Electrochem. Sci.,* 8 (2013) 12860.
40. The wealth of India, *NISCAIR press publishers New Delhi*, (2006) 305.
41. N.P. Sahu, S.B. Mahto and R.N. Chakravarti, *Ind j pharm***.** 12 (1974) 284.